

<https://doi.org/10.1038/s41538-025-00404-z>

Indole compounds from fermented soybean products activate the aryl hydrocarbon receptor to reduce liver injury



Yanyun Wang^{1,6}, Leping Quan^{2,6}, Xiaomin Zheng³, Qiang Hu¹, Xiaoli Huang⁴, Yang Pu⁴, Guangfa Xie^{1,5}✉ & Qi Peng²✉

The consumption of stinky tofu, a traditional fermented soybean product from China, elevates the concentrations of indole and trimethylindole in murine feces and increases the levels of indole in serum, as well as indole in the liver. These hepatic compounds act as ligands for the Aryl Hydrocarbon Receptor (AHR), triggering activation of this receptor, which subsequently enhances the expression of the enzyme cytochrome P450 (CYP) 1A1. This upregulation diminishes the levels of pro-inflammatory cytokines, thereby attenuating alcohol-induced liver injury. This study underscores the potential of dietary indole from stinky tofu to mitigate Alcoholic liver disease (ALD), laying a foundation for the development of functional foods and novel treatment strategies for ALD.

Fermented foods, globally recognized for their extended shelf life and distinctive flavors, are produced through the actions of microorganisms. These microbial processes not only degrade harmful substances in food but also suppress pathogenic bacteria and generate an array of beneficial metabolites, thereby positioning fermented foods as functional foods¹. Research indicates that microbial fermentation can degrade insecticide residues, such as pyrethroids, and enhance antioxidant capacity through the fermentation of compounds like the polysaccharides from “*Polygonum cuspidatum*”, which also improves the intestinal microbiota and boosts immunity in mice. Yi et al. discovered that buffalo yogurt fermented with *Lactobacillus plantarum* has the potential to lower blood pressure in pregnant hypertensive rats²⁻⁴. Stinky tofu, a traditional Chinese fermented soy product, is characterized by its potent aroma derived from indole and sulfide compounds, produced through microbial action on tofu⁵. Despite its popularity, research has predominantly focused on its flavor and processing techniques, with limited exploration into its functional properties. The Aryl Hydrocarbon Receptor (AHR), a ligand-dependent intracellular receptor protein, is ubiquitously present in the liver, spleen, lymph nodes, and other vertebrate tissues⁶. The AHR is activated by a diverse range of ligands, which can be categorized into exogenous and endogenous types. Exogenous AHR ligands, or their

precursors, originate externally and include compounds such as resveratrol, commonly found in dietary sources. Conversely, endogenous ligands are primarily products of tryptophan metabolism within the organism, facilitated by intestinal microorganisms. Notable among these metabolites are indole, indole-3 acetic acid, and indole-3 acetaldehyde, all of which serve as ligands for AHR⁷. Recent studies have demonstrated that the AHR can bind to dietary AHR ligands, intestinal microbial metabolites, and host-derived authigenic metabolites, initiating the transcription of downstream target genes and thus regulating various bodily functions. For instance, research has indicated that jujube A can activate AHR and mitigate symptoms of polycystic ovary syndrome (PCOS). Additionally, Jing discovered that berberine can activate the AHR receptor to ameliorate colitis, further underscoring the therapeutic potential of AHR activation^{8,9}. The indole compound derived from stinky tofu functions as a ligand for the AHR. Investigating its capacity to activate the AHR receptor *in vivo* represents a significant area of research interest. Alcohol ranks among the top causes of preventable diseases and mortality globally, as well as a primary factor in liver disease. Alcoholic liver disease (ALD), induced by excessive alcohol consumption, stands as a foremost cause of chronic liver pathology worldwide and is prevalent among severe liver conditions¹⁰. The phenotypic manifestations of ALD

¹College of Life Science, Leshan Normal University, Leshan, China. ²National Engineering Research Center for Chinese CRW (branch center), School of Life and Environmental Sciences, Shaoxing University, Shaoxing, China. ³Wuxi Maternity and Child Health Care Hospital, Affiliated Women's Hospital of Jiangnan University, Wuxi, China. ⁴Shaoxing Testing Institute of Quality and Technical Supervision, Shaoxing, China. ⁵Zhejiang Collaborative Innovation Center for Full-Process Monitoring and Green Governance of Emerging Contaminants, College of Biology and Environmental Engineering, Zhejiang Shuren University, Hangzhou, China. ⁶These authors contributed equally: Yanyun Wang, Leping Quan. ✉e-mail: 3582123211@qq.com; xiegf@zjsru.edu.cn; dr_pengqi@163.com

are diverse, ranging from hepatic steatosis to hepatitis, fibrosis, and in certain cases, progression to cirrhosis and hepatocellular carcinoma¹¹. Alcohol metabolism triggers lipid accumulation and inflammatory responses in the liver¹². Currently, the management of ALD is limited to abstinence from alcohol, nutritional support, and prevention of cirrhosis. Consequently, there is a pressing need to identify effective pharmaceutical treatments and programs to mitigate and manage the progression of ALD¹³. This study investigates the potential of stinky tofu's foodborne indoles, particularly as AHR ligands, to impact fecal, serum, and hepatic levels and assesses their role in activating the AHR pathway and mitigating ALD. The findings could inform the development of functional foods and therapeutic strategies for ALD.

Results

Analysis of nutritional properties of stinky tofu

Nutritional quality is a critical characteristic of food, especially for fermented products such as stinky tofu, which is celebrated for its distinctive flavor and health benefits. This study analyzed the nutritional content of unfermented tofu and stinky tofu, revealing significant differences attributable to fermentation. The energy content was lower in stinky tofu (1013.91 kJ/100 g) compared to unfermented tofu (1176.64 kJ/100 g) (Fig. 1A). Similarly,

reductions were observed in the fat and protein contents of stinky tofu, with protein showing the most substantial decrease (Fig. 1B, C). These reductions are linked to the metabolic activities of microorganisms that consume macronutrients in the tofu during fermentation. Free amino acids serve not only as taste components in food but also as crucial indicators of its nutritional properties. Comparative analysis revealed that the amino acid content in stinky tofu was higher than in regular tofu. This variation can be attributed to microbial metabolism, which affects amino acid levels in two primary ways. Firstly, microorganisms decompose proteins present in food to release free amino acids. Secondly, microorganisms can autonomously synthesize specific amino acids. Both mechanisms contribute to an elevated amino acid content in fermented foods, as demonstrated in Fig. 1D. Moreover, Microbes play a crucial role as regulators of bodily health. The study found that the levels of certain vitamins—riboflavin, cobalamin, and thiamine were significantly higher in stinky tofu than in unfermented tofu, whereas niacin levels remained unchanged (Fig. 1E). The ability of microorganisms, particularly lactic acid bacteria, to synthesize vitamins during fermentation is well documented. For instance, lactic acid bacteria enhance riboflavin levels in fermented sourdough, and similar fermentative actions promote cobalamin synthesis during grain fermentation. Likewise, fermentation by *Lactobacillus plantarum* has been shown to increase thiamine

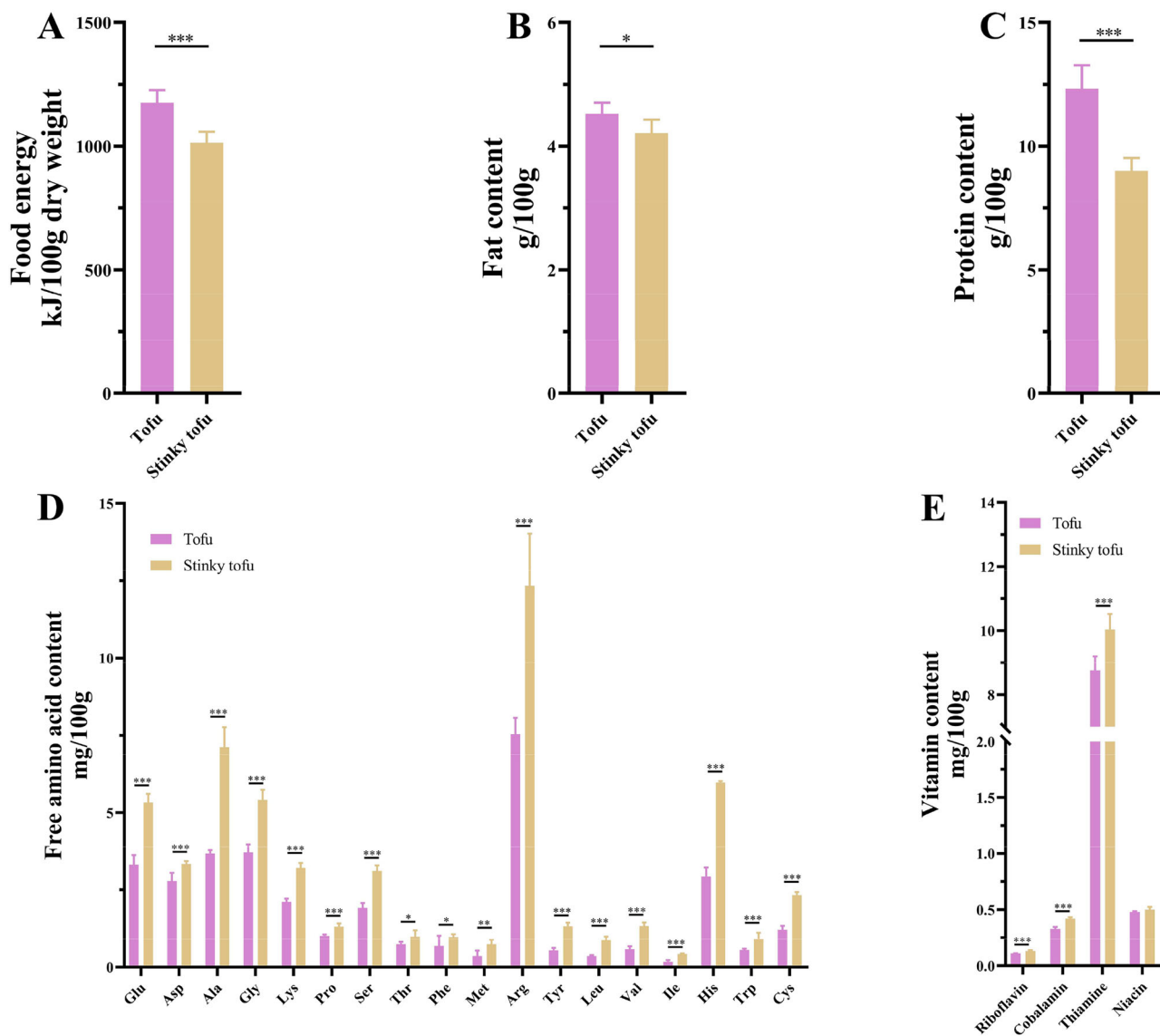


Fig. 1 | Nutritional analysis of tofu and stinky tofu. A Comparison of energy levels between tofu and stinky tofu. B Fat content in tofu and stinky tofu. C Protein content in tofu and stinky tofu. D Free amino acid levels in tofu and stinky tofu. E Vitamin content in tofu and stinky tofu.

content in *Polygonati Rhizoma*^{14–16}. In conclusion, the fermentation of tofu into stinky tofu not only modifies its macro-nutrient content by reducing levels of energy, fat, and protein but also enhances its micro-nutrient profile by increasing amino acids and essential vitamins. These findings highlight the dual role of microbial fermentation in diminishing certain nutritional elements while enriching others, thus improving the overall nutritional properties of the food.

Stinky tofu increased fecal indole and trimethylindole levels

The microbial metabolism of protein in stinky tofu not only enhances its flavor profile but also results in the formation of significant quantities of indole and 3-methylindole. Analytical results indicated that the indole concentration in stinky tofu was substantially higher at 6307.45 µg/g compared to a mere 54.93 µg/g in unfermented tofu. Similarly, the concentration of 3-methylindole was 3738.70 µg/g in stinky tofu, as opposed to only 16.52 µg/g in unfermented tofu (Fig. 2A). These findings underscore stinky tofu's rich content of indole and trimethylindole, highlighting its potential as a source of food-borne indoles. In an experimental setting using SPF BALB/c mice, the influence of stinky tofu on the fecal concentrations of tryptophan metabolites was investigated. Mice fed with stinky tofu (AlcST group) exhibited significantly higher levels of indole and trimethylindole in their feces compared to those in the control (Ctrl) and alcohol (Alc) groups fed with unfermented tofu. Previous research has documented that such metabolites are typically produced by the action of intestinal microorganisms on tryptophan¹⁷. In this study, with the exception of indole and trimethylindole, significant differences were observed in other tryptophan metabolites across all groups. To minimize the impact of additional nutrients, present in stinky tofu, the excretion levels of indole and trimethylindole in AlcIN mice, which were fed these compounds, were elevated compared to those in Alc mice. This suggests that while stinky tofu did not alter the tryptophan metabolism by intestinal microorganisms, it directly increased the concentrations of indole and trimethylindole in the gut (Fig. 2B). Furthermore, it has been reported that indole-3-carbinol, another derivative of indole, acts as a ligand for the AHR and is prevalent in brassica vegetables. Increased intake of such vegetables has been associated with elevated levels of AHR ligands¹⁸. This correlation suggests a similar potential mechanism by which stinky tofu

could enhance AHR ligand availability through its high indole and trimethylindole content.

Foodborne indole increases the level of liver AHR ligand

Indole and trimethylindole, after being ingested, can be absorbed into the bloodstream from the intestine. Our analysis showed that consumption of stinky tofu significantly enhanced serum indole levels (Fig. 3A). Specifically, the serum indole levels in the AlcIN group were notably higher than those observed in the Ctrl and Alc groups. While serum trimethylindole levels were slightly elevated in the AlcST and AlcIN groups compared to Ctrl and Alc groups, these changes were statistically significant (Fig. 3B). The greater increase in serum indole levels, compared to trimethylindole, may be attributed to the smaller molecular size of indole, which facilitates easier passage through the intestinal barrier, and the less efficient intestinal accumulation of trimethylindole. Upon entering the bloodstream, indole is transported to the liver via the hepatic artery. Once in the liver, indole is metabolized into indoxyl by the enzyme CYP2E2, and subsequently, indoxyl is transformed into Indoxyl sulfate through the catalytic action of SULT1A1. The resulting Indoxyl sulfate is then transported out of the liver via the portal vein to the kidneys, where it is excreted in the urine. Analysis of liver samples revealed that the concentrations of indole in the AlcST and AlcIN groups were significantly higher than those in the other study groups, indicating that dietary intake of indole can lead to its accumulation in the liver. However, the levels of indoxyl in the liver of the AlcST and AlcIN groups did not differ significantly, although there was a general increase in Indoxyl sulfate levels across these groups (Fig. 3C–E). This suggests differential metabolic handling of indole derivatives within the liver, influenced by dietary factors. Furthermore, the expression levels of CYP2E1 and SULT1A1, the enzymes responsible for converting indole into indole sulfate, were elevated in the AlcST and AlcIN groups. This upregulation suggests that indole accumulation may enhance the synthesis of indole sulfate in the liver to some extent (Fig. 3F, G). Indoxyl sulfate is one of the important ways in which the liver metabolizes indole, and the increase of indoxyl sulfate synthesis may help to avoid the excessive accumulation of indole in the liver¹⁹. Typically, such enzymatic intermediates maintain a dynamic equilibrium in the body, thus preventing the build-up of intermediate products like indoxyl. Indole and its metabolite, indole sulfate, are recognized as ligands for the AHR. Studies have demonstrated that indole ameliorates liver inflammation via the AHR pathway, and indole sulfate, within certain

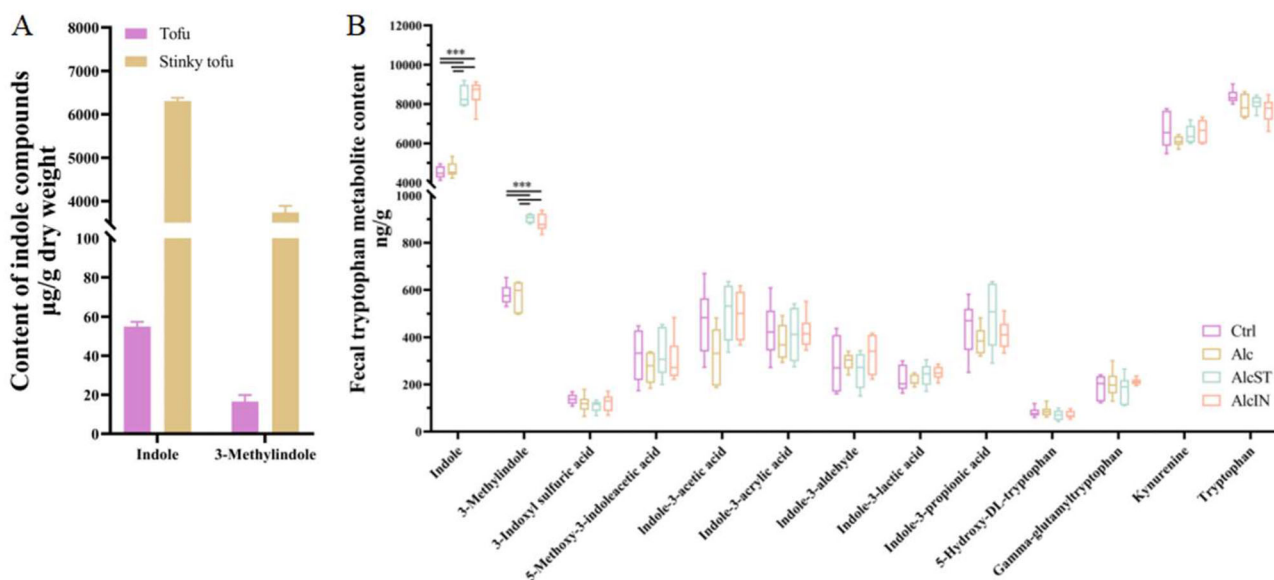


Fig. 2 | Influence of stinky tofu on fecal indole and related metabolites. A Indole levels in tofu and stinky tofu. **B** Concentrations of indoles and related metabolites in feces from mice fed tofu and stinky tofu.

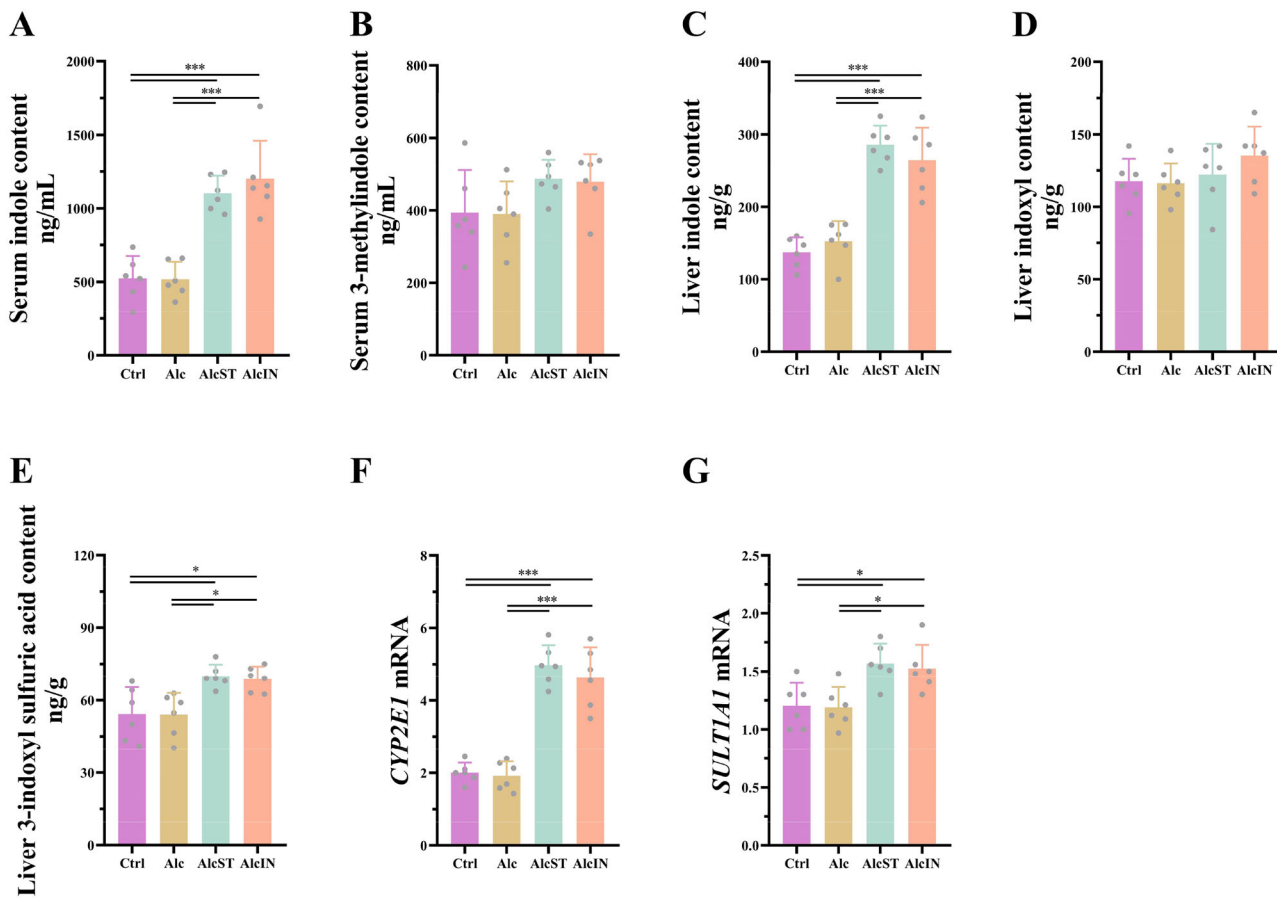


Fig. 3 | Impact of stinky tofu on indole and its metabolites in vivo. **A** Serum indole content in mice fed tofu and stinky tofu. **B** Serum 3-methylindole content in mice fed tofu and stinky tofu. **C** Liver indole content in mice fed tofu and stinky tofu. **D** Liver indoxyl content in mice fed tofu and stinky tofu. **E** Liver 3-indoxyl sulfate content in

mice fed tofu and stinky tofu. **F** Expression level of CYP2E1 in the liver of mice fed tofu and stinky tofu. **G** Expression level of SULT1A1 in the liver of mice fed tofu and stinky tofu.

doses, can modulate astrocyte activity²⁰. Therefore, the observed increase in AHR ligands in the liver due to dietary indole intake likely influences the AHR signaling pathway, suggesting a beneficial role in the hepatic response to inflammatory stimuli.

Activation of liver AHR receptor promotes the expression of CYP1A1

The AHR is also ubiquitously present in the liver, functioning as a nuclear transcription regulatory factor. Indole and indole sulfate serve as ligands for AHR. Activation of AHR can directly influence the expression of its target genes and several downstream genes. The expression of CYP1A1 is primarily regulated by AHR, making it one of the key target genes of the AHR receptor²¹. CYP1A1, a key enzyme in the cytochrome P450 family, plays a central role in the oxidative metabolism of a wide range of endogenous and exogenous compounds, including alcohol and its toxic metabolites. In the liver, CYP1A1 is involved in the detoxification process by metabolizing reactive compounds such as acetaldehyde, a major byproduct of alcohol metabolism. The activation of CYP1A1 through the AhR pathway has been linked to enhanced detoxification processes, which may reduce the overall toxic burden on hepatocytes during alcohol consumption. In our study, we observed that the activation of the AhR pathway by foodborne indole compounds from fermented soy products resulted in upregulation of CYP1A1 expression, which we propose as one of the key mechanisms by which these compounds attenuate alcohol-induced liver damage. By reinforcing the liver's ability to metabolize and detoxify harmful byproducts of alcohol,

CYP1A1 acts as a protective enzyme that reduces the extent of hepatocyte damage and supports liver regeneration. In this study, it was observed that the expression levels of CYP1A1 were significantly elevated in the AlcST and AlcIN groups (Fig. 4A). Unlike CYP1A1, CYP1A2, another enzyme in the cytochrome P450 family, did not show a significant difference in expression across the groups²², illustrating that AHR activation does not uniformly affect all its target genes. This observation aligns with findings from studies in other species, such as pigs exposed to β-naphthoflavone, where CYP1A1 expression was increased without a corresponding increase in CYP1A2²³. Additionally, AHR repressor (AHRR), which serves as a feedback inhibitor of AHR, was also found to have increased expression in the AlcST and AlcIN groups, indicating a robust activation of the AHR signaling pathway (Fig. 4C). To further validate whether the observed upregulation of CYP1A1 was directly due to AHR activation, the specific AHR antagonist CH-223191 was employed. This antagonist inhibits the TCDD-mediated nuclear translocation of AHR and its binding to DNA²⁴. The results indicated that both excrement and serum indole levels in the AlcSTCH group were elevated, and the liver concentrations of indole and indole sulfate also increased to a certain extent. This suggests that the availability of AHR ligands in the liver of mice in the AlcSTCH group was sufficient (Fig. 4D-G). However, despite these increases, the expression levels of the CYP1A1 gene did not rise, nor did the expression of the AHRR gene, which is regulated by AHR. The use of CH-223191 inhibited the regulatory effects of AHR, substantiating that the upregulation of hepatic CYP1A1 was driven by AHR activation (Fig. 4H, L).

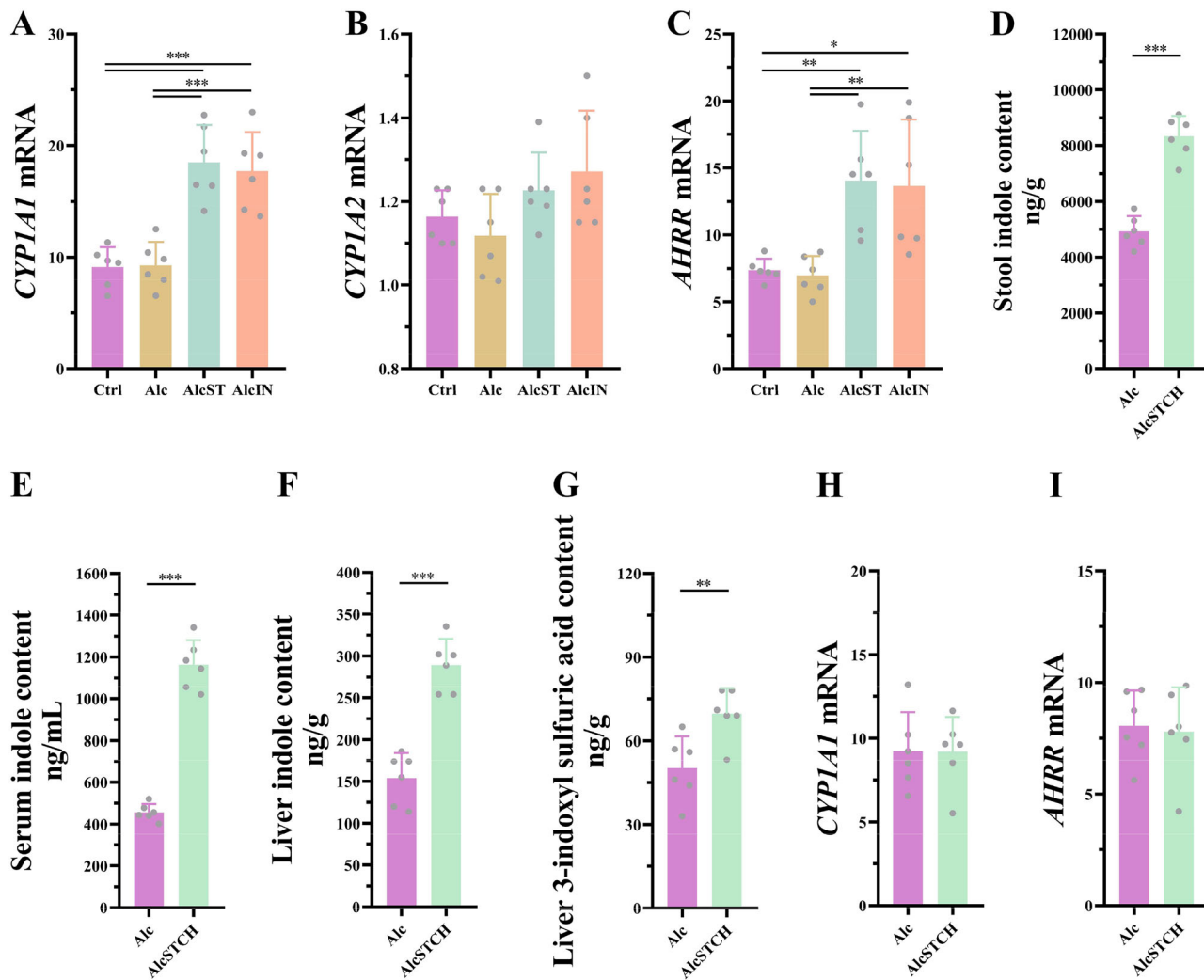


Fig. 4 | Influence of stinky tofu on liver AHR receptor target genes. **A** *CYP1A1* expression levels in the liver of mice fed tofu and stinky tofu. **B** *CYP1A2* expression levels in the liver of mice fed tofu and stinky tofu. **C** *AHRR* expression levels in the liver of mice fed tofu and stinky tofu. **D–I** Indole content and gene expression in the

liver of AlcSTCH mice fed stinky tofu: **D** Fecal indole content. **E** Serum indole content. **F** Liver indole content. **G** Liver 3-indoxyl sulfate content. **H** *CYP1A1* expression level. **I** *AHRR* expression level.

Foodborne indole activates the liver AHR pathway to alleviate ALD

Alcohol consumption can lead to liver steatosis and hepatitis, collectively contributing to the development of ALD. The progression of ALD is intricately linked with the AHR pathway²⁵. In this study, pathological analysis revealed that, compared to the Ctrl group, the Alc group exhibited blurred liver cords, enlarged hepatocytes, steatosis, and mild inflammatory infiltration—hallmark features of ALD. In the AlcST and AlcIN groups, the liver architecture appeared clearer, and hepatocyte enlargement was observed with minimal to no inflammatory infiltration, indicating an alleviation of ALD in these groups (Fig. 5A). Biochemical analysis of serum revealed elevated levels of ALT and AST in the Alc, AlcST, and AlcIN groups compared to Ctrl. However, levels in the AlcST and AlcIN groups were significantly lower than in the Alc group. Serum TC and TG were also assessed, showing significantly higher levels in the Alc group compared to others, with no marked differences between the AlcST and AlcIN groups and the Ctrl group (Fig. 5B–E). SCD1, a crucial gene involved in the synthesis of monounsaturated fatty acids within the liver, plays a significant role in lipid metabolism. Elevated expression of SCD1 has been associated with increased fat accumulation and obesity²⁶. In our study, expression levels of SCD1 in the Alc, AlcST, and AlcIN groups were elevated compared to the Ctrl group. Notably, the levels in the AlcST and AlcIN groups were

significantly lower than those in the Alc group, suggesting that the consumption of foodborne indoles mitigates the upregulation of the SCD1 gene induced by ALD and the resultant hepatic lipid accumulation (Fig. 5F). This finding aligns with existing research indicating that a reduction in SCD1 expression may ameliorate ethanol-induced liver injury²⁷. ALD not only precipitates hepatic steatosis but also incites inflammation. Chemokines such as CCL2 and tumor necrosis factors (TNFs) play pivotal roles in orchestrating these inflammatory responses. Alcohol consumption elevates the expression of chemokine CCL2, whereas foodborne indoles mitigate this effect. For chemokine CCL3, significant upregulation was observed in the Alc group, whereas the AlcST and AlcIN groups did not exhibit a marked increase in expression levels. Similarly, the expression of tumor necrosis factor-alpha (TNF- α) was significantly higher in the Alc group compared to other groups, while TNF- α levels in the AlcST and AlcIN groups did not show significant elevations. Expression of tumor necrosis factor beta (TNF- β) was upregulated in all groups; however, the increase was less pronounced in the AlcST and AlcIN groups relative to the Alc group.

Interleukin-1 beta (IL-1 β) is another critical mediator of the inflammatory process, with alcohol consumption leading to increased expression. Indoles derived from food sources were found to counteract this rise in IL-1 β expression. Transforming Growth Factor beta (TGF- β), a key promoter of hepatitis and liver fibrosis, exhibited a similar pattern: its overexpression

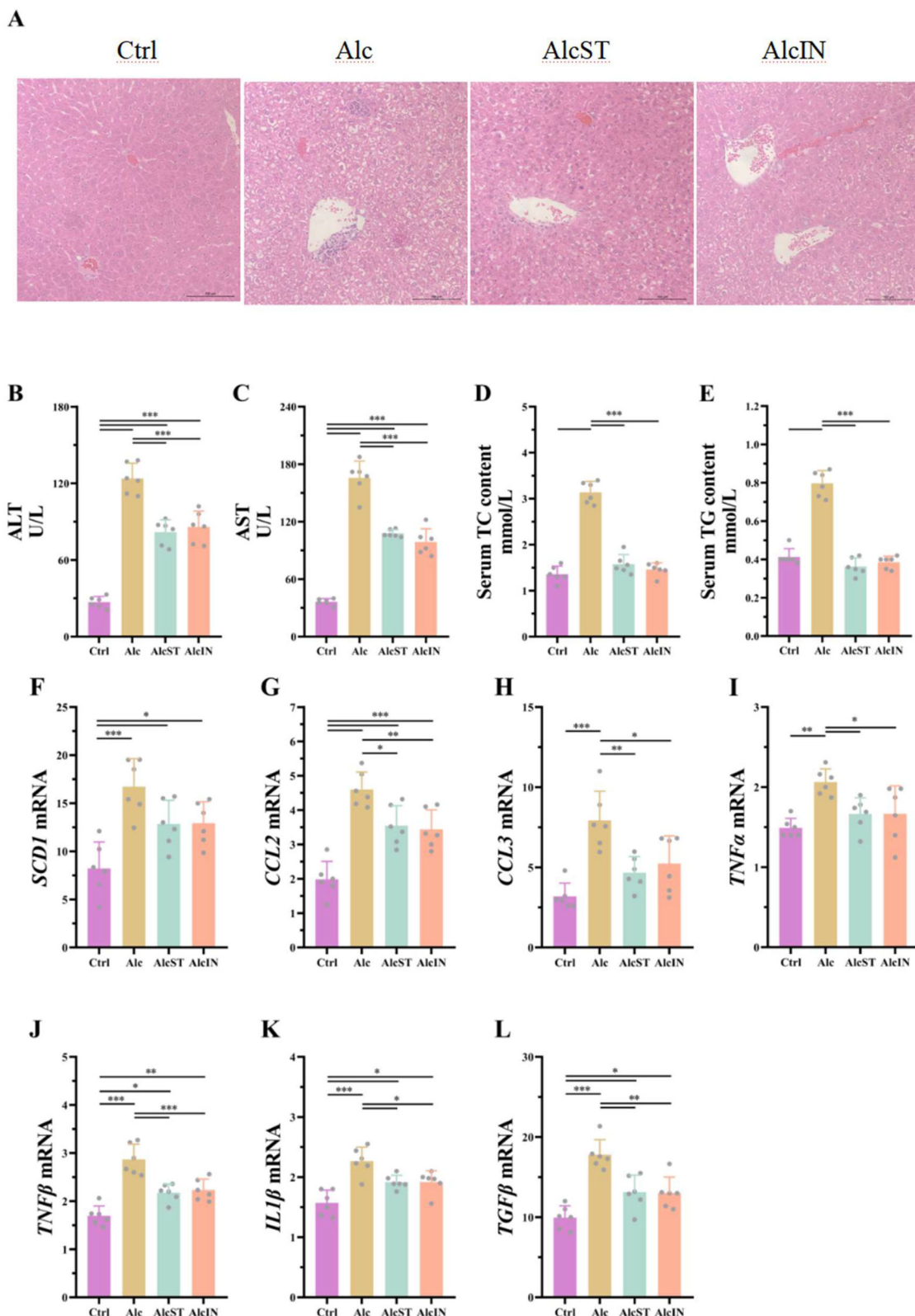


Fig. 5 | Effects of stinky tofu on alcoholic liver disease (ALD). A H&E staining of liver sections from different groups. B–E Serum biochemical analyses (ALT, AST, TC, TG) across different groups. F–L Gene expression analysis related to lipid metabolism and inflammation in the liver.

induced by alcohol was attenuated by foodborne indoles (Fig. 5G–L). We acknowledge the important role of AHR expression not only in hepatocytes but also in other liver cell types, such as immune cells and hepatic stellate cells (HSCs). AHR activation in immune cells like macrophages and

dendritic cells plays a crucial role in reducing inflammation in liver injury²⁸. Additionally, AHR activation in HSCs has been shown to inhibit their activation, thereby mitigating fibrosis^{29,30}. Our study indicates that indole compounds, by activating the AHR pathway, may modulate both immune

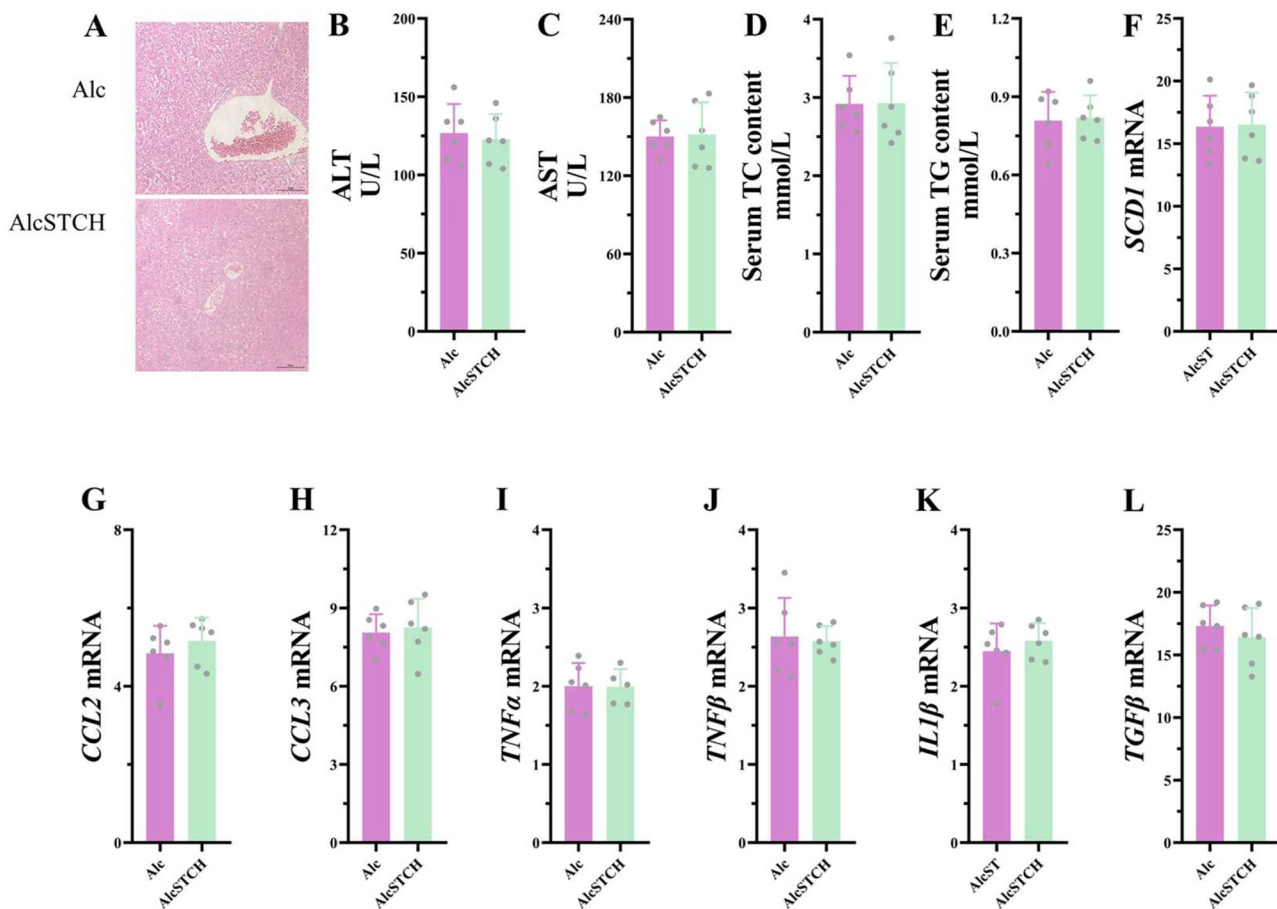


Fig. 6 | Impact of stinky tofu on ALD in AlcSTCH mice. **A** Liver H&E staining results showing tissue morphology. **B–E** Serum analysis for ALT, AST, TC, and TG in AlcSTCH mice. **F–L** Gene expression related to lipid metabolism and inflammation in the liver of AlcSTCH mice.

responses and fibrogenic processes, contributing to the protection against liver damage. This evidence underscores the potential therapeutic effects of dietary indoles in modulating inflammatory markers associated with alcoholic liver disease. Additionally, this study examined the effects of ALD in the AlcSTCH group mice, revealing that these mice exhibited liver cell edema, inflammatory infiltration, and steatosis (Fig. 6A). When compared with the Alc group, there was no significant reduction in serum levels of ALT, AST, TC, and TG, nor was there a noticeable decrease in the levels of chemokines CCL2 and CCL3, TNF- α and TNF- β , IL-1 β , or TGF- β (Fig. 6B–L). This observation suggests that when the AHR is inhibited, foodborne indoles lose their capacity to mitigate ALD. In conclusion, the mediation of the AHR pathway by dietary indoles is crucial for the alleviation of alcoholic liver disease.

Discussion

Stinky tofu is a traditional fermented soybean product in China, which has a unique flavor. Its microbial metabolism produces a large number of indole compounds. In a murine model study, it was observed that dietary intake of these foodborne indoles from stinky tofu significantly elevated the concentrations of indoles and trimethylindoles in feces, as well as indole levels in serum. These findings underscore the impact of dietary components on metabolite profiles in biological systems. Indole functioning as ligands for the AHR, activated the AHR pathway in the liver. This activation enhanced the expression of the AHR target gene CYP1A1, which is crucial for the metabolic processing of various substances. Concomitantly, there was a notable reduction in the expression levels of inflammation-related factors, contributing to the mitigation of alcoholic liver injury. This research not only confirms the protective effects of foodborne indole against ALD but also underscores the potential of stinky tofu and similar fermented foods in

the development of functional foods aimed at treating or preventing ALD. Thus, foodborne indoles from stinky tofu represent a promising avenue for the dietary management of liver disease, providing a foundational reference for future therapeutic strategies.

Methods

Sample collection and determination of routine nutritional indexes

Stinky tofu samples and unfermented tofu samples were procured from Hangzhou Bean Food Co Ltd. Upon collection, samples were immediately frozen and stored at -80°C until analysis. The caloric content of the samples was determined using the combustion calorimetry technique³¹. Specifically, A 1 g sample, freeze-dried and finely ground, was accurately weighed and subjected to analysis using the KL-12Mn (PRECYZJA-BIT, Poland) bomb calorimeter. The combustion heat of the sample was determined based on the change in water temperature surrounding the calorimetric bomb and the precise weight of the sample. The results were automatically calculated by the calorimeter software, with the energy content expressed per 100 g of dry weight. For the determination of fat content, samples were analyzed according to the GB 5009.6-2016 National Food Safety Standard using the Soxhlet extraction method. Protein content was quantified following the GB 5009.5-2016 National Food Safety Standard using the Kjeldahl nitrogen determination method.

Analysis of free amino acids and vitamins

To determine the free amino acid content, 5 g of each sample was accurately weighed and homogenized with 50 mL of ultra-pure water, followed by ultrasonication at 50°C for 40 min. The homogenate was then centrifuged at $10,000 \times g$ for 15 min. The supernatant was filtered through a $0.22 \mu\text{m}$

microporous filter and adjusted to a final volume of 50 mL with ultra-pure water. For the preparation of the analysis sample, 100 μ L of the filtered solution was mixed with 250 μ L of acetonitrile, vortexed, and centrifuged at 10,000 $\times g$ for 3 min. A 10 μ L aliquot of the supernatant was transferred to a sample vial, to which 70 μ L of AccQ buffer (Waters, USA) and 20 μ L of AccQ-Tag derivatization reagent (Waters, USA) were added. The mixture was then heated at 55 °C for 10 min prior to analysis. Amino acid standards were derivatized in the same manner. Chromatographic separation was performed using a Waters ACQUITY UPLC FLR System equipped with an AccQ-Tag TM Ultra column (2.1 mm \times 100 mm). Chromatographic Conditions: The chromatographic analysis employed four mobile phases: Mobile Phase A consisted of AccQ-Tag Ultra A eluent; Mobile Phase B was composed of 10% *v/v* AccQ-Tag Ultra B eluent (water to AccQ-Tag Ultra B ratio of 90:10); Mobile Phase C utilized water; Mobile Phase D used AccQ-Tag Ultra B eluent. The flow rate was maintained at 0.7 mL/min, with the column temperature set at 35 °C and the sample compartment temperature at 20 °C. The injection volume was 10 μ L, and the detection wavelength was set at 260 nm. Elution Protocol: The elution was conducted according to the following gradient program: at time 0 min, 2% A, 0% B, 98% C, 0% D; at 5.49 min, 9% A, 80% B, 11% C, 0% D; at 7.10 min, 8% A, 15.6% B, 57.9% C, 18.5% D; at 7.69 min, 7.8% A, 0% B, 70.9% C, 21.3% D; at 7.99 min, 4% A, 0% B, 36.3% C, 59.7% D; at 8.68 min, 2% A, 0% B, 98% C, 0% D; at 10.2 min, 2% A, 0% B, 98% C, 0% D. Each injection cycle was 10 min. Quantification of Free Amino Acids: The content of free amino acids in the samples was quantified using an external standard method. The concentrations were calculated based on a standard curve established from standard samples.

Vitamin content was determined using a high-performance liquid chromatography (HPLC) method. A 0.5 g sample was accurately weighed and homogenized with 70 mL of ultra-pure water. The mixture was sonicated at 90 °C for 30 min, cooled, and diluted to 100 mL with ultra-pure water. The sample was then shaken and filtered into a sample solution. The analysis was conducted using an Agilent 1260 HPLC system equipped with a Hypersil C18 column (250 mm \times 4.0 mm, 5 μ m). The column temperature was maintained at 35 °C. The mobile phase consisted of a phosphate buffer with a pH of 3.0 (0.01 mol/L KH_2PO_4 , 0.005 mol/L sodium octane sulfonate, 0.5% triethylamine) and methanol, mixed in a volume ratio of 75:25. The flow rate was set at 1.0 mL/min, with UV detection at 275 nm and an injection volume of 20 μ L. Vitamin content was quantified using the external standard method and calculated according to the standard calibration curve.

Preparation of feed

Tofu and stinky tofu samples were first freeze-dried and then ground into fine particles. The powders were sterilized via irradiation to ensure microbiological safety before use. The processed stinky tofu powder was incorporated into experimental feed formulations by Jiangsu Xietong Pharmaceutical Bio-engineering Co. Ltd, China. The final concentration of stinky tofu powder in the feed was set at 6.35%, which corresponds to an indole content of 0.4 mg/g and a trimethylindole content of 0.24 mg/g. Based on an average daily feed intake of 5 g per mouse, this formulation provides daily intakes of 2 mg of indole and 1.2 mg of trimethylindole. For the control group, additional freeze-dried tofu powder was added to the maintenance feed to achieve a final concentration of 5.47% by weight. This adjustment was made to match the caloric contribution of the stinky tofu feed. A separate tofu feed was also prepared by adding indole and trimethylindole to standard tofu feed at concentrations of 0.4 mg/g and 0.24 mg/g, respectively, to assess the effects of these compounds independently of the fermentation process.

Animals and experimental scheme

This study utilized BALB/c strain, SPF-grade male mice. Animals were housed in groups of three to five per cage under controlled conditions with ad libitum access to feed and water. The facility maintained a 12-hour light/dark cycle (lights on from 08:00 to 20:00), with ambient temperature

regulated between 21 °C and 24 °C and relative humidity between 40% and 70%. Prior to the commencement of the experimental protocols, mice were acclimatized to these conditions with standard feed for one week to ensure adaptation. Following an adaptation period, the mice were allocated into five distinct groups, each comprising ten mice: the Ctrl group received a tofu diet; the Alc group was fed a tofu diet supplemented with ethanol; AlcST: Mice were fed a basal diet supplemented with 6.35% stinky tofu powder, equivalent to a daily intake of indole (2 mg) and 3-methylindole (1.2 mg) based on 5 g of feed per mouse; AlcIN: Mice were fed a tofu-based diet with added indole (0.4 mg/g) and 3-methylindole (0.24 mg/g) to match the indole levels in the AlcST group; the AlcSTCH group received a stinky tofu diet combined with ethanol and CH-223191 (Sigma-Aldrich, China). CH-223191 was intraperitoneally injected daily at a dose of 10 mg/kg. Each dietary regimen was designed to assess the impact of different components on hepatic health.

In addition to their regular feed, the experimental mice were subjected to a daily gavage of 200 μ L. Specifically, during the initial week, the Alc group, AlcST group, AlcIN group, and AlcSTCH group received 5% (*v/v*) ethanol via gavage. The ethanol concentration was incrementally increased over the week, reaching 50% (*v/v*) by week's end. In contrast, the Ctrl group was administered an equivalent daily dose of a maltodextrin suspension, calibrated to match the energy content of the ethanol concentration. From the second week through the sixth week, the Alc group, AlcST group, AlcIN group, and AlcSTCH group continued to receive 50% (*v/v*) ethanol via gavage. Concurrently, the Ctrl group received a daily gavage of a maltodextrin suspension whose energy content was equivalent to that of 50% (*v/v*) ethanol. At the conclusion of the sixth week, all mice were anesthetized. The anesthetic used was pentobarbital at a dose of 50 mg/kg (mouse body weight), administered via intraperitoneal injection, subsequently euthanized for sample collection, adhering to humane endpoints. All animal procedures were conducted in compliance with the institutional guidelines for the care and use of laboratory animals, approved by the Ethical Review Board (animal certificate number: SCXK (Jiangsu) 2021-0056). All animal experiments comply with the ARRIVE guidelines and should be carried out in accordance with the U.K. Animals (Scientific Procedures) Act, 1986, and associated guidelines, EU Directive 2010/63/EU for animal experiments.

Analysis of indole and its derivatives

Fecal, Serum, liver, and food samples preparation: samples were prepared by weighing 100 mg (50 mg for food samples) and freeze-drying under vacuum. Each sample was homogenized in 850 μ L of 100% methanol (800 μ L for serum and liver samples) using a homogenizer set at 65 Hz for 3 min. After centrifugation at 15,000 $\times g$ for 10 min at 4 °C, the supernatant was collected and vacuum-dried at 45 °C for 3 h. The dry residue was resuspended in 100 μ L of 10% methanol solution (methanol:water = 1:9, *v/v*), followed by final centrifugation at 15,000 $\times g$ for 10 min at 4 °C. The clear supernatant was then filtered through a 0.22 μ m microporous filter membrane. The analysis of indole derivatives was performed according to the methodology outlined by Fang³². The detection utilized an ultra-high performance liquid chromatography (UHPLC) system coupled with a Q Exactive Fourier transform mass spectrometer (Thermo Fisher, CA, USA). For chromatographic separation, 2 μ L of each prepared sample was injected into a BEH C18 column, measuring 100 mm by 2.1 mm with a particle size of 1.7 μ m. The mobile phases were water with 0.1 formic acid (A) and acetonitrile/isopropanol (1:1) with 0.1% formic acid (B). The gradient profile was as follows: 0 min, 5% B; 3 min, 20% B; 9 min, 95% B; 13 min, maintained at 95% B; 13.1 min, reverted to 5% B; and held until 16 min. The flow rate was 0.40 mL/min, and the column temperature was set at 40 °C. Detection was performed in positive ion mode, with an ion source heating temperature of 400 °C and an ionization voltage of 3500 V. Quantification was based on external standards with calibration curves derived from standard samples.

Table 1 | Primers used in this study

Gene name	Upstream primer (5' → 3')	Downstream primer (5' → 3')
IL1 β	TGAGGACATGAGCACCTTC	GGGAACGTCACACACCA
TGF β	TCCCTAACCTCAAATTATTCA	GCGGTCCACCATTAGCAC
TNF α	TGGGAGTAGACAAGGTACAACCC	CATCTCTCAAATTGAGTGACAA
TNF β	TGTTGGCCTCACACCTTCAG	AATTGTTGCTCAABGAGAAACCA
CCL2	AGGTCCCTGTATGCTTCTG	TCTGGACCCATTCTCTTGTG
CCL3	TCTGCCACCTGCATAG	TGAAGAGTCCCTCGATGTG
SCD1	CCGGAGACCCCTAGATCGA	TAGCTGTAAAAGATTCTGCAAA
CYP1A1	CATCACAGACAGCCTATTGAGC	CTCCACGAGATAGCAGTTGTGAC
CYP1A2	CAGTGGTACAGATGGCGTTCTC	GCAGTGGCCAGTAGCAGCTC
AHRR	ACATACGCCGGTAGGAAGAGA	ACATACGCCGGTAGGAAGAGA
CYP2E1	CTTGCAGGAACAGAGACCA	ATGCACTACAGCGTCCATGT
SULT1A1	TGAGACGCACTCACCCGTCT	TCCAGTCTCTCAGGTAGAG
GAPDH	CGTCCCGTAGACAAAATGGT	TTGATGGCAACAATCTCCAC

Determination of serum biochemical indices

Blood samples were collected and allowed to clot at room temperature for 2 h, followed by centrifugation at 3000 \times g for 15 min. The serum was isolated for biochemical analysis. Alanine aminotransferase (ALT), aspartate aminotransferase (AST), total cholesterol (TC), and triglycerides (TG) were measured using standard biochemical kits (Nanjing Jiancheng Bioengineering Institute, China).

Histopathological analysis

Liver tissues were rinsed with saline, fixed in 4% paraformaldehyde for 24 h, and subsequently embedded in paraffin. Sections of 5 μ m thickness were cut and stained with Hematoxylin and Eosin (H&E) for histological examination.

Total RNA extraction and RT-qPCR analysis

Samples were frozen and pulverized in liquid nitrogen. Total RNA was extracted using Trizol reagent (Invitrogen, USA), with nuclease inhibitors added to prevent RNA degradation. RNA integrity was confirmed by 1% agarose gel electrophoresis and quantified using a NanoDrop2000 spectrophotometer (Thermo Fisher, USA). RNA samples were reverse-transcribed into cDNA using the PrimeScriptTM FAST RT reagent Kit with gDNA Eraser (Takara, Japan). Quantitative PCR (qPCR) was performed using TB Green[®] Premix Ex Taq[™] II (Tli RNaseH Plus) on a CFX96 Touch DeepWell (Bio-Rad, USA), with GAPDH serving as the internal control (Table 1). Relative gene expression was calculated using the 2^{-ΔΔCt} method.

Statistical analysis

Data compilation and preliminary graphical analyses were conducted using Microsoft Excel 2019 and GraphPad Prism software version 8.0, respectively. Statistical analyses were performed with IBM SPSS Statistics software version 26.0. All experimental procedures were replicated six times, and results are presented as mean \pm standard deviation (SD). To assess the distribution of the data, the Shapiro-Wilk test was employed to verify normality. For comparisons between two groups, data following a normal distribution were analyzed using the student's *t*-test, while the Mann-Whitney *U*-test was applied to data that did not exhibit normal distribution. For comparisons among multiple groups with a normal distribution, a one-way ANOVA was utilized. Statistical significance was set at * P < 0.05, ** P < 0.01, *** P < 0.001, indicating increasing levels of significance.

Data availability

The datasets used and/or analyzed during the current study are available from the corresponding author upon reasonable request.

Code availability

Inapplicability.

Received: 11 July 2024; Accepted: 3 March 2025;

Published online: 24 March 2025

References

- Skowron, K. et al. Two faces of fermented foods—the benefits and threats of its consumption. *Front. Microbiol.* **13**, 17 (2022).
- Yu, X. et al. Microbial fermentation as an efficient method for eliminating pyrethroid pesticide residues in food: a case study on cyfluthrin and *Aneurinibacillus aneurinilyticus* D-21. *J. Agric. Food Chem.* **72**, 4393–4404 (2024).
- Li, Y. C. et al. *Polygonatum odoratum* fermented polysaccharides enhance the immunity of mice by increasing their antioxidant ability and improving the intestinal flora. *Food Biosci.* **58**, 14 (2024).
- Yi, L. et al. Buffalo yogurt fermented with commercial starter and *Lactobacillus plantarum* originating from breast milk lowered blood pressure in pregnant hypertensive rats. *J. Dairy Sci.* **107**, 62–73 (2024).
- Tang, H. et al. The formation mechanisms of key flavor substances in stinky tofu brine based on metabolism of aromatic amino acids. *Food Chem.* **392**, 12 (2022).
- Gutiérrez-Vázquez, C. & Quintana, F. J. Regulation of the immune response by the aryl hydrocarbon receptor. *Immunity* **48**, 19–33 (2018).
- Safe, S. et al. Aryl hydrocarbon receptor (AHR) ligands as selective AHR modulators (SAhRMs). *Int. J. Mol. Sci.* **21**, 16 (2020).
- Zhou, N. et al. Jujuboside A attenuates polycystic ovary syndrome based on estrogen metabolism through activating AhR-mediated CYP1A2 expression. *Reprod. Sci.* **12**, 2234–2245 (2024).
- Jing, W. H. et al. Berberine improves colitis by triggering AhR activation by microbial tryptophan catabolites. *Pharmacol. Res.* **164**, 14 (2021).
- Gao, B. & Bataller, R. Alcoholic liver disease: pathogenesis and new therapeutic targets. *Gastroenterology* **141**, 1572–1585 (2011).
- Chacko, K. R. & Reinus, J. Spectrum of alcoholic liver disease. *Clin. Liver Dis.* **20**, 419–427 (2016).
- Dunn, W. & Shah, V. H. Pathogenesis of alcoholic liver disease. *Clin. Liver Dis.* **20**, 445–456 (2016).
- Suk, K. T., Kim, M. Y. & Baik, S. K. Alcoholic liver disease: treatment. *World J. Gastroenterol.* **20**, 12934–12944 (2014).
- Llamas-Arriba, M. G. et al. Lactic acid bacteria isolated from fermented doughs in spain produce dextrans and riboflavin. *Foods* **10**, 20 (2021).

15. Ashagrie, H. et al. Cereal-based fermented foods as a source of folate and cobalamin: the role of endogenous microbiota. *Food Res. Int.* **174**, 12 (2023).
16. Wang, Z. L. et al. Insights into the metabolic profiling of polygonati rhizoma fermented by *Lactiplantibacillus plantarum* under aerobic and anaerobic conditions using a UHPLC-QE-MS/MS system. *Front. Nutr.* **10**, 13 (2023).
17. Lu, Y. et al. TrpNet: understanding tryptophan metabolism across gut microbiome. *Metabolites* **12**, 16 (2022).
18. Popolo, A. et al. Two likely targets for the anti-cancer effect of indole derivatives from cruciferous vegetables: PI3K/Akt/mTOR signalling pathway and the aryl hydrocarbon receptor. *Semin. Cancer Biol.* **46**, 132–137 (2017).
19. Tennoune, N., Andriamihaja, M. & Blachier, F. Production of indole and indole-related compounds by the intestinal microbiota and consequences for the host: the good, the bad, and the ugly. *Microorganisms* **10**, 15 (2022).
20. Beaumont, M. et al. The gut microbiota metabolite indole alleviates liver inflammation in mice. *Faseb J.* **32**, 6681–6693 (2018).
21. Mescher, M. & Haarmann-Stemmann, T. Modulation of CYP1A1 metabolism: from adverse health effects to chemoprevention and therapeutic options. *Pharmacol. Ther.* **187**, 71–87 (2018).
22. Zhou, S. F. et al. Insights into the substrate specificity, inhibitors, regulation, and polymorphisms and the clinical impact of human cytochrome P450 1A2. *Aaps J.* **11**, 481–494 (2009).
23. Messina, A. et al. Expression and inducibility of CYP1A1, 1A2, 1B1 by β-naphthoflavone and CYP2B22, 3A22, 3A29, 3A46 by rifampicin in the respiratory and olfactory mucosa of pig. *Toxicology* **260**, 47–52 (2009).
24. Kim, S. H. et al. Novel compound 2-methyl-2H-pyrazole-3-carboxylic acid (2-methyl-4-o-tolylazo-phenyl)-amide (CH-223191) prevents 2,3,7,8-TCDD-induced toxicity by antagonizing the aryl hydrocarbon receptor. *Mol. Pharmacol.* **69**, 1871–1878 (2006).
25. Wrzosek, L. et al. Microbiota tryptophan metabolism induces aryl hydrocarbon receptor activation and improves alcohol-induced liver injury. *Gut* **70**, 1299–1308 (2021).
26. Li, F. et al. Lipidomics reveals a link between CYP1B1 and SCD1 in promoting obesity. *J. Proteome Res.* **13**, 2679–2687 (2014).
27. Lounis, M. A. et al. SCD1 deficiency protects mice against ethanol-induced liver injury. *Biochim. Biophys. Acta Mol. Cell Biol. Lipids* **1861**, 1662–1670 (2016).
28. Paludan, S. R., Bowie, A. G., Horan, K. A. & Fitzgerald, K. A. Recognition of herpesviruses by the innate immune system. *Nat. Rev. Immunol.* **13**, 143–154 (2013).
29. Tai, W. T. et al. Discovery of novel Src homology region 2 domain-containing phosphatase 1 agonists from sorafenib for the treatment of hepatocellular carcinoma. *Hepatology* **65**, 2135 (2017).
30. Segeritz, C. P. et al. hiPSC hepatocyte model demonstrates the role of unfolded protein response and inflammatory networks in α₁-antitrypsin deficiency. *J. Hepatol.* **69**, 851–860 (2018).
31. Reder, M. et al. The application of FT-MIR spectroscopy for the evaluation of energy value, fat content, and fatty acid composition in selected organic oat products. *Food Anal. Meth.* **7**, 547–554 (2014).
32. Fang, Z. et al. Bifidobacterium longum mediated tryptophan metabolism to improve atopic dermatitis via the gut-skin axis. *Gut Microbes* **14**, 2044723 (2022).

Acknowledgements

This work was supported by the Zhejiang Shaoxing Huangjiu Industry Innovation Service Complex-Technological Innovation Project in Zhejiang Province (no. 2023KJ082); the Foundation of Public Projects of Zhejiang Province, China (no. LGN22C200008); the Program Foundation of Public Projects of Shaoxing city, Zhejiang Province, China (no. 2018C30010); the Foundation of Public Projects of Zhejiang Province, China (no. 2017C32101); the Shaoxing University Fund (No.08021066); the Shaoxing University Fund (no. 08220102213); the Shaoxing University Fund (no. 08240102300); and the Leshan Normal University “Scientific Research Cultivation Project” (no. KYPY2024-T002). We would like to thank Huajun Zheng for their important contributions to the preliminary data collection for this study.

Author contributions

Yanyun Wang: writing-review and editing, investigation, data curation, and methodology. Leping Quan: investigation, data curation, and visualization. Xiaomin Zheng: data curation and visualization. Qiang Hu: investigation and data curation. Xiaoli Huang: investigation and methodology. Yang Pu: investigation, data curation, and visualization. Guangfa Xie: supervision, visualization, and funding acquisition. Qi Peng: supervision, project administration, and funding acquisition.

Competing interests

All authors declare no competing interests.

Additional information

Correspondence and requests for materials should be addressed to Guangfa Xie or Qi Peng.

Reprints and permissions information is available at <http://www.nature.com/reprints>

Publisher's note Springer Nature remains neutral with regard to jurisdictional claims in published maps and institutional affiliations.

Open Access This article is licensed under a Creative Commons Attribution-NonCommercial-NoDerivatives 4.0 International License, which permits any non-commercial use, sharing, distribution and reproduction in any medium or format, as long as you give appropriate credit to the original author(s) and the source, provide a link to the Creative Commons licence, and indicate if you modified the licensed material. You do not have permission under this licence to share adapted material derived from this article or parts of it. The images or other third party material in this article are included in the article's Creative Commons licence, unless indicated otherwise in a credit line to the material. If material is not included in the article's Creative Commons licence and your intended use is not permitted by statutory regulation or exceeds the permitted use, you will need to obtain permission directly from the copyright holder. To view a copy of this licence, visit <http://creativecommons.org/licenses/by-nc-nd/4.0/>.

© The Author(s) 2025